Journal of Neuroscience Research 87:1219–1229 (2009)

Characterization of Periinfarct Flow Transients With Laser Speckle and Doppler After Middle Cerebral Artery Occlusion in the Rat

Janos Luckl,[1] Chao Zhou,[2] Turgut Durduran,[2] Arjun G. Yodh,[2] and Joel H. Greenberg[1]*

[1]Department of Neurology, University of Pennsylvania, Philadelphia, Pennsylvania
[2]Department of Physics and Astronomy, University of Pennsylvania, Philadelphia, Pennsylvania

Little information exists on the role and the characteristics of perfusion changes related to periinfarct depolarization. Our aim was to visualize and monitor periinfarct flow transients (PIFTs) in Sprague-Dawley rats (n = 10) with two different laser methods in a closed-skull model of filament middle cerebral artery occlusion. A laser Doppler probe was placed over the ischemic cortex 5 mm lateral to Bregma, and a 5 × 5 mm area centered 5 mm posterior and 4 mm lateral to Bregma was thinned for laser speckle imaging. Both neurological and histological evaluations were performed at 72 hr postinjury. Mean flow during 90-min ischemia was 29% of baseline measured by laser Doppler and 36–54% by laser speckle. Flow transients occurred in all rats, the number of PIFTs being 4.6 ± 1.8/90 min. By both methods, 95.6% of them occurred with temporal correlation. The average duration of PIFTs was also identical (162 ± 24 and 162 ± 34 sec, respectively). Five different morphologies of flow transients ranging from hypoperfusive to hyperemic were identified by laser speckle. The PIFTs changed their morphology dynamically over certain regions. All of the animals showed an infarct (178.5 ± 26 mm^3) in the middle cerebral artery territory. Laser Doppler in itself can be a reliable method for counting/detecting PIFTs, but laser speckle is capable of monitoring the dynamic changes in PIFT morphology over the penumbral and periischemic cortex.

Key words: focal ischemia; intraluminal suture model; isoflurane; optical imaging

Spreading depression (SD) is a response of the central nervous system to different noxious stimuli. In his original demonstration with the rabbit brain, Leao showed that the depolarization event propagating throughout the cortical field was hyperemic (Leao et al., 1944). Most studies support a biphasic hemodynamic change in SD, with a large hyperperfusion shortly after the direct current potential shift followed by a long-lasting hypoperfusion (Goadsby et al., 1992; Seitz et al., 2004). Some studies also report that, before the hyperemic phase, there is a transient hypoperfusion (Dreier et al., 2001; Ayata et al., 2004). Both hypoxia and hypotension can change the morphology of the flow transients (Sukhotinsky et al., 2008), and in addition there is a species difference in which vasoconstrictive coupling was observed during SD in mice but not in adult rat with laser Doppler (LD) flowmetry (Ayata et al., 2004).

Transient increases in extracellular potassium ion concentration within the ischemic penumbra were first described following middle cerebral artery (MCA) occlusion in baboons (Branston et al., 1977) and cats (Strong et al., 1983). The properties of these potassium ion changes have been elucidated by many research groups, and their designation as periinfarct depolarizations (PIDs) has been widely accepted (Hossmann, 1996). In focal ischemia, the blood flow responses to PIDs are highly polymorphic when monitored with laser speckle (LS). Strong and colleagues (2007) observed five different patterns of flow transients in cats, and Shin and colleagues (2006) reported repetitive PIDs associated with hypoperfusion in the penumbral tissue of mice subjected to MCA occlusion, with episodic hypoperfusion followed by hyperemia in the nonischemic cortex (Shin et al., 2006). LD studies in the rat show that hyperemic flow transients are linked to the passage of direct current deflections (Iijima et al., 1992), and this increase in blood flow is proportional to the residual flow (Nallet et al., 2000). Similarly, the flow data collected in our laboratory by one or two LD probes at different recording sites in the ischemic cortex of rats indicate that the

Contract grant sponsor: NIH; Contract grant number: NS30785 and NS057400 (to J.H.G.); Contract grant sponsor: University of Pennsylvania.

*Correspondence to: Joel H. Greenberg, PhD, Department of Neurology, University of Pennsylvania, 415 Stemmler Hall, 3450 Hamilton Walk, Philadelphia, PA 19104-6063. E-mail: joel@mail.med.upenn.edu

Received 20 June 2008; Revised 4 September 2008; Accepted 10 September 2008

Published online 11 November 2008 in Wiley InterScience (www.interscience.wiley.com). DOI: 10.1002/jnr.21933

flow transients are mostly hyperemic events (70–90%) and do not show regional heterogeneity in morphology. The discrepancy between the predominately hyperemic flow transients observed with LD during MCA occlusion in the rat and the suggestion of polymorphic flow transients from the studies of Strong et al. (2007) and Shin et al. (2006) prompted us to use a technique with high spatial resolution (LS contrast imaging) to test our hypothesis that flow transients are mostly hyperemic in rats and do not show regional heterogeneity.

MATERIALS AND METHODS

MCA Occlusion

All procedures performed were approved by the Institutional Animal Care and Use Committee of the University of Pennsylvania. Adult male Sprague-Dawley rats (290–340 g) were anesthetized with 4% isoflurane for induction in a mixture of 50% nitrous oxide and 50% oxygen. Body temperature was monitored by a rectal probe and maintained at 37.2°C ± 0.5°C with a heating blanket regulated by a homeothermic blanket control unit (Harvard Apparatus Limited, Holliston, MA). A polyethylene catheter (PE-50) was placed into the tail artery for the measurement of arterial blood pressure and for blood gas sampling. Blood pressure was continuously monitored using a pressure transducer and recorded with a computer-based recording system (PowerLab; ADInstruments, Colorado Springs, CO). The rats were placed into a stereotaxic headholder, and the head was prepared for monitoring of changes in cerebral blood flow. An LD probe was placed over the ischemic cortex 5 mm lateral to Bregma, and a 5 × 5 mm area centered 5 mm posterior and 4 mm lateral to Bregma was thinned for LS imaging (Fig. 1). We are aware that the variation of skull thickness could influence the value of measured relative blood flow changes (Parthasarathy et al., 2008). Therefore, special attention was paid during surgical preparation to make the skull thickness uniform. Additionally, the simultaneous use of two laser methods might conceivably result in differences in flow values. However, in separate studies exploring the simultaneous use of LD and LS, we have found that the LS yields a nonsignificantly (1.5% ± 3%) higher flow if the LD laser is on, and the LS laser does not influence the LD recordings.

Transient focal cerebral ischemia was induced using the filament model as previously used from our laboratory (Shimazu et al., 2005), modified slightly to accommodate the imaging apparatus. With the animal in a supine position, a midline neck incision was made, and the right external and internal carotid arteries were dissected from the surrounding connective tissue. A 4.0 nylon monofilament suture coated with silicone (Doccol Corporation, Redlands, CA) was inserted into the right common carotid artery (CCA) and advanced about 9–10 mm into the right ICA. The animals were returned to the stereotaxic headholder, and optical imaging was started. After the surgical preparation, isoflurane was maintained at 1.2% in a 70:30 mixture of nitrous oxide and oxygen in each animal during ischemia, with 1.4% isoflurane administered for a short period (2 min) during the occlusion to blunt the painful surgical stimuli to the animal's neck. At the desired time, the filament was gently advanced until LD flowmetry indicated adequate MCA occlusion by a sharp decrease in ipsilateral blood flow to 15–25% of baseline. After 90 min of occlusion, the suture was withdrawn to allow for cerebral reperfusion. Samples for blood gas (arterial pH, PaO_2, and $PaCO_2$) and glucose analysis were taken from the tail artery catheter prior to and during the ischemic period and measured with a blood analyzer (i -STAT; Heska Corporation, Fort Collins, CO).

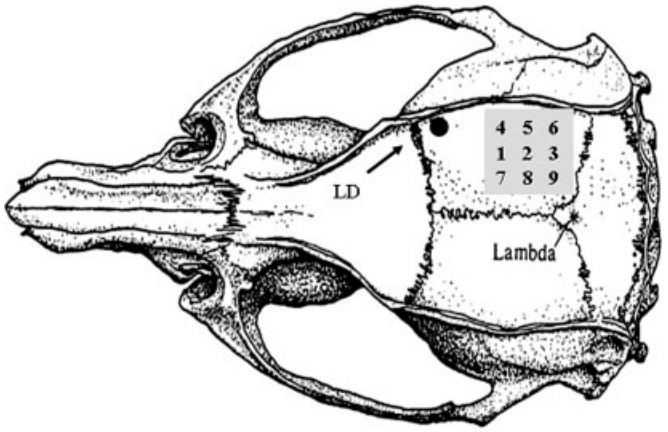

Fig. 1. The experimental setup with the recording site (full circle) of the laser Doppler probe (LD) and the layout of the nine regions of interest (ROI). The gray area represents the approximate position and size of the thinned skull for laser speckle imaging. Modified from Paxinos and Watson (1982).

After the end of acute monitoring, the scalp suture was closed. The arterial catheter was withdrawn, all wounds were closed, and the animals were placed into their cages, where they were allowed free access to food and water.

LS Flowmetry: Image Acquisition and Postprocessing

A collimated laser diode (Hitachi HL 785 1G, 785 nm, 50 mW; Thorlabs, Newton, NJ) driven by a custom-made driver illuminated the thinned skull at approximately 30–40° from vertical. One percent hydroxycellulose gel topped with cover glass was used to minimize the surface reflection from the skull. The laser beam was adjusted to provide uniform illumination of the surface of the skull. Images were recorded by a 12-bit, TEC cooled CCD camera (Uniq; Uniq Vision Inc.) using imaging software (StreamPix; NorPix, Montreal, Quebec, Canada). A 60-mm lens (Schneider-Kreuznach, Apo-Componon 2.8/40, Germany) was used to focus the image, and the aperture was adjusted so that the speckle size matched the pixel dimensions (9.9 × 9.9 μm). The camera was externally triggered at 10 Hz using the digital output of an A/D board (DataWave Technologies, Boulder, CO) over the duration of MCA occlusion. The exposure time for each frame was set to 1/120 sec. A 7 × 7 sliding window was employed to calculate speckle contrast images, from which cerebral blood flow (CBF) maps were extracted (Briers, 2001) as described previously (Dunn et al., 2001; Durduran et al., 2004). In this formulation, the correlation time (τ_c), which is

inversely proportional to the mean velocity of the scattering particles, relates to the speckle contrast (C) and the camera exposure time (T):

$$C = \frac{\sigma}{\langle I \rangle} = \left[\frac{\tau_c}{2T} \left(1 \quad e^{\frac{-2T}{\tau_c}} \right) \right]^{1/2}.$$

Relative changes in CBF are assumed to be proportional to the mean velocity. As noted by Wang et al. (2007), there are no significant discrepancies in relative blood flow measurements using this formulation compared with the formula described by Goodman (1985) and Bandyopadhyay et al. (2005). Ten CBF images were averaged to improve the signal-to-noise ratio further, resulting in an effective CBF frame rate of 1 Hz.

Relative CBF images were obtained by normalizing the CBF images with baseline measurements obtained at the beginning of the data collection with a correction for biological zero (CBF values when cerebral perfusion was zero; Ayata et al., 2004; Strong et al., 2006; Zhou et al., 2008). In this study, biological zero images could not be obtained in each animal because the animals were not sacrificed until days after the imaging. Consequently, a separate group (n = 6) was used to determine the biological zero value, which was found to be 8.2% ± 1.4%. Nine circular regions of interests (ROIs, 1 mm in diameter; Fig. 1) were evenly spaced on the image, avoiding vessels, for the analysis of periinfarct flow transients (PIFTs) and blood flow changes.

PIFTs were identified by their propagating feature (PIFT seen in at least two ROIs with appropriate time delay). The start and the end of the PIFT were determined by the time at which the average laser speckle signal, which was obtained as the mean 1 min both prior to and following a PIFT, intercrossed with the ascending or the descending leg of PIFTs (Fig. 2). The amplitude was obtained as the percentage change in CBF, both the hypoperfusion and hyperemia components of the amplitudes measured separately. The percentage of different morphologies of the PIFTs was calculated from the total number of PIFT over each ROI. Propagation speed of the flow transients was obtained from the time difference between peaks at the different ROI locations.

LD Flowmetry

An LD probe (tip diameter 1 mm; fiber separation 0.25 mm) attached to a flowmeter (PeriFlux 4001; Perimed Stockholm, Sweden) was affixed over a 1-mm-diameter circular area of thinned skull rostral to the LS measurement area using super glue to obtain a continuous measure of relative CBF during the experiment. The initial drop and the average flow during ischemia (90 min) and reperfusion (15 min) were calculated as a percentage of the baseline (10 min) prior to MCA occlusion. A separate group was used to determine biological zero for LD, which was found to be 3.2% ± 1.0%. Criteria for identifying PIFTs were the following (Luckl et al., 2008): 1) flow transient with amplitude greater than 5% of baseline; 2) duration of blood flow change longer than 60 sec; and 3) stable blood pressure during the event. The parameters (duration, positive and negative peaks of the amplitude) of the PIFTs were measured by the principles we applied in the LS flowmetry.

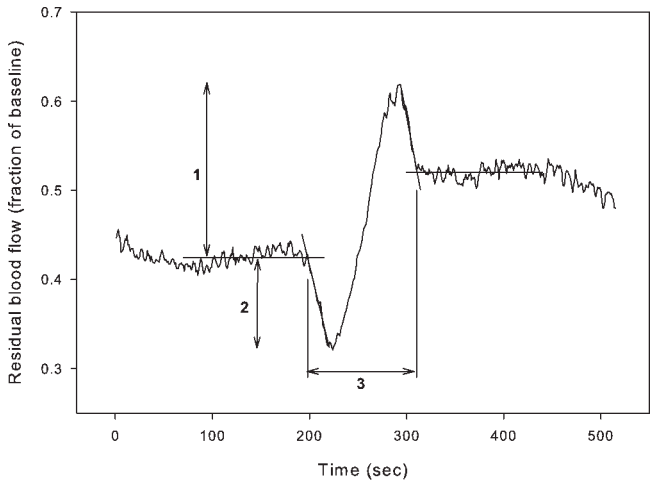

Fig. 2. A typical type II periinfarct flow transient (PIFT). The start and the end of the PIFT were determined by the time at which the mean laser Doppler or laser speckle signal intercrossed with the ascending and the descending legs of the PIFT. Duration (line 3) is the elapsed time between the start and the end of the PIFT. The positive (line 1) and negative (line 2) peaks of the amplitude were expressed as a percent change in CBF from the pretransient mean.

Neurological Evaluation and Infarct Volume Measurement

A neurological evaluation was performed at 72 hr postinjury according to the protocol of Belayev et al. (1996). Postural reflex, visual placing in forward and sideways directions, tactile placing of the dorsal and lateral paw surfaces, and proprioceptive placing were tested and scored on a 12-point scale ranging from 0 (no deficit) to 12 (maximum deficit).

Rats were sacrificed 72 hr after MCAO. The brain was removed from the skull and sectioned in the coronal plane at 2-mm intervals using a rodent brain matrix. The brain slices were stained with 2% triphenyltetrazolium chloride (TTC) and photographed, and the infarct size was determined as described previously (Burnett et al., 2006). This provided data on the severity of the ischemic insult in each animal and permitted confirmation of a successful occlusion.

Statistical Analysis

Changes in the physiological parameters (baseline and intraischemic) were tested by paired *t*-test. A two-way ANOVA analysis was performed to test for differences in blood flow between ROIs during baseline and during ischemia and any regional differences in distribution of PIFT types. Correlations between the parameters of PIFTs, CBF, infarct size, and neurological outcome were evaluated using linear regression analysis. Statistical significance was considered at $P < 0.05$. Data are expressed as mean ± SD.

TABLE I. The physiological variables (n = 10) during baseline (15. min. prior MCAO) and ischemia (20–30. min. after MCAO). Data are mean ± SD.

	BP (mmHg)	T core (°C)	pH	pC02 (mmHg)	p02 (mmHg)
Baseline	103 ± 11	37.2 ± 0.2	7.45 ± 0.02	36.5 ± 2.4	109 ± 13
Ischemia	123 ± 10	37.6 ± 0.3	7.42 ± 0.02	41.0 ± 2.6	111 ± 11

T: temperature; BP: blood pressure

TABLE II. Mean Residual Blood Flow, Reperfusion, Duration, and Peak Amplitudes of Periinfarct Flow Transients (PIFT) Over Regions of Interest*

ROI	CBF ischemia (% of baseline)	CBF reperfusion (% of baseline)	PIFT duration (sec)	Positive peak amplitude (% change)	Negative peak amplitude (% change)
LD	29 ± 9	118 ± 46	162.0 ± 34.0	11.0 ± 2.9	8.7 ± 1.3
4	42 ± 15	111 ± 28	163.3 ± 19.4	7.2 ± 3.5	9.5 ± 6.2
5	36 ± 10	88 ± 20	167.5 ± 19.1	7.5 ± 4.3	10.5 ± 5.2
6	42 ± 10	72 ± 20	161.9 ± 27.2	10.2 ± 6.1	10.8 ± 5.8
1	38 ± 11	93 ± 24	148.9 ± 25.7	6.1 ± 3.4	8.4 ± 5.2
2	39 ± 9	78 ± 18	153.9 ± 26.2	7.7 ± 3.3	10.5 ± 4.1
3	39 ± 10	65 ± 13	183.3 ± 42.7	10.2 ± 6.3	10.3 ± 5.8
7	47 ± 11	88 ± 26	155.0 ± 37.8	14.9 ± 10.5	10.4 ± 6.7
8	50 ± 10	76 ± 20	162.8 ± 41.8	14.5 ± 11.7	11.5 ± 7.1
9	54 ± 14	80 ± 21	170.0 ± 39.1	18.3 ± 11.3	12.6 ± 5.3

*All data (except reperfusion CBF) averaged over 90 min of ischemia, mean ± SD. Reperfusion CBF averaged over 15 min. CBF, cerebral blood flow; ROI, regions of interest; LD, site of laser Doppler. See Figure 1 for locations of ROIs.

RESULTS

Physiological Variables

All of the physiological parameters were within normal limits both during the surgical preparation and during MCAO (Table I). With the exception of pO_2, all of the physiological variables during ischemia are significantly different ($P < 0.05$) from the baseline (preischemic) values, but they are in the normal range.

LS Flowmetry

We did not find any heterogeneity or directional trend during baseline flow measurements ($P > 0.1$). The mean flow values averaged over the 90 min of ischemia ranged between 36% and 54% by LS (Table II) over the nine ROIs. The mean residual flow in the medial row (ROI 7, 8, 9; see Fig. 1) was statistically higher than the flow both in the middle row (ROI 1,2,3; $P < 0.001$) and in the lateral row ($P < 0.002$), but there was no anterior-posterior heterogeneity in ischemic flow ($P = 0.54$). LS did not show an evolving CBF deficit. The reperfusion was complete in each animal; the averaged flow over the first 15 min of reperfusion in each ROI is summarized in Table II. The mean number of PIFTs detected with LS was 4.6 ± 1.8/90 min, identical to that with LD; 95.6% of them were temporally correlated (Fig. 3). The average duration of PIFTs ranged between 148.9 ± 25.7 sec and 183.3 ± 42.7 sec over the multiple ROIs, comparable to the duration by LD (Table II). The pretransient baseline and the average amplitude of the positive and negative peaks both show a strong, positive correlation measured by LS ($P < 0.0001$) over each region of interest (Fig. 4). The balance (positive peaks – negative peaks) of the averaged amplitudes is positive (3.0–5.8%) over the anterior cerebral artery (ACA)-medial cerebral artery watershed zone (ROI 7, 8, 9), whereas the balance is negative (–0.1% to –3.2%) over the ''pure'' MCA territory (ROI 1–6).

We could distinguish five different morphologies of flow transients by LS (Fig. 5): I) monophasic, hyperemic; II, III) biphasic (hyperemia or hypoperfusion dominant); and IV, V) monophasic, hypoperfusive (transient or prolonged). Events were categorized as ''PIFT with nonidentifiable morphology'' if an almost ''flat'' line over the flow registration site or an obscured morphology was seen over 1–7 ROIs whereas a well-defined morphology (types I–V) was seen time correlated at least over two ROIs. The occurrence of these events over the nine ROIs is summarized in Table III.

There were 414 events in the nine ROIs (10 animals) over 90 min of observation. Eighteen events (4.3%), however, were excluded because of problems inherent to the data collection scheme. We did not find any correlations between the different morphologies of the PIFTs and the ischemic (pretransient) flow.

Type I: Monophasic, Hyperemic Flow Transients

This flow transient is characteristic for the medial parasagittal ribbon of the cortex, where its occurrence is 55–64% (Table III, Fig. 5). We consider this part of the cortex as periischemic. The occurrence of type I was greater in this region than in regions more laterally ($P < 0.01$). The mean flow values were 47% ± 11%, 50% ± 10%, and 54% ± 14% of baseline over these ROIs.

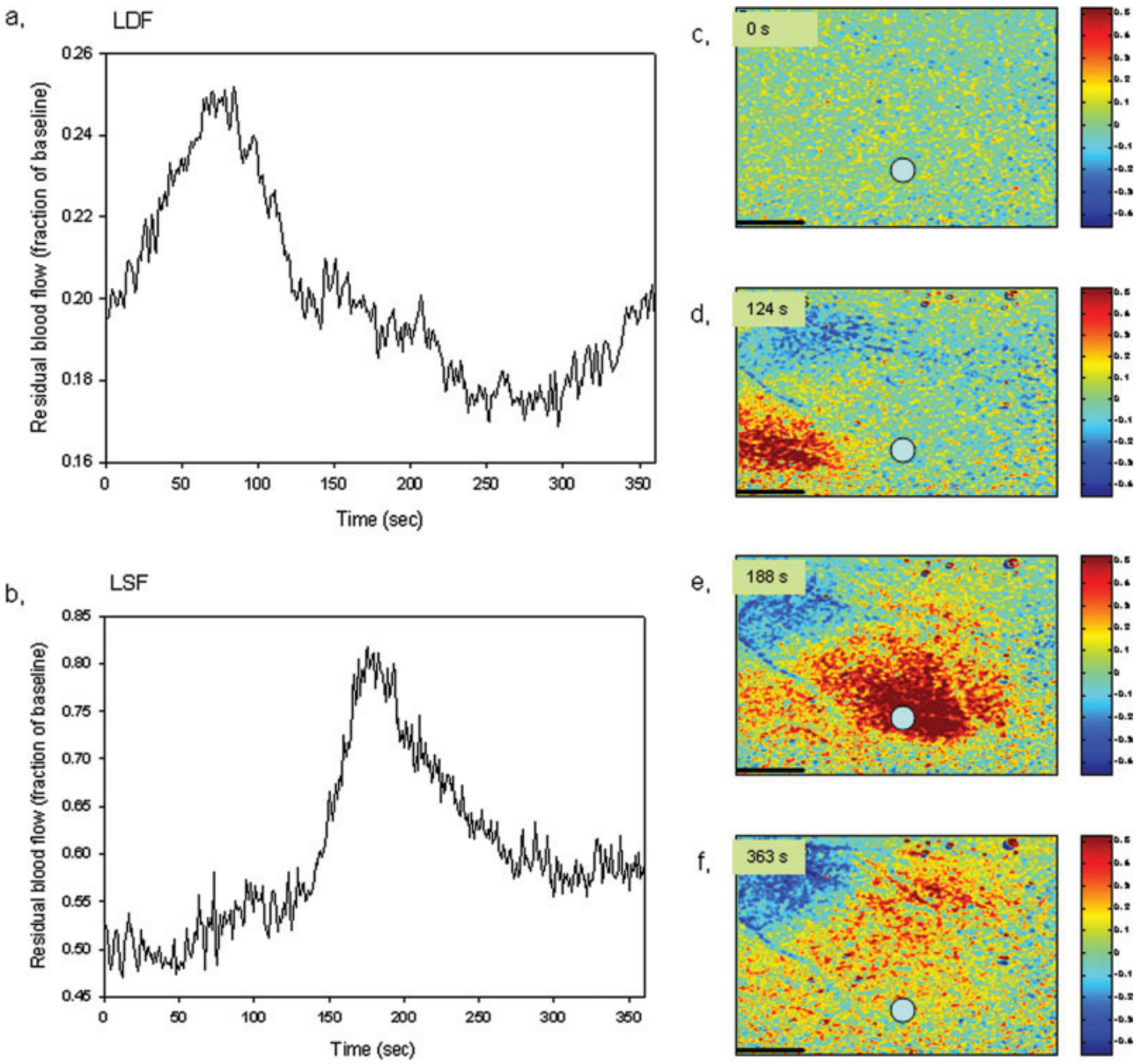

Fig. 3. Anteroposterior propagation of periinfarct flow transients (**c–f**) detected by both laser Doppler (**a**) and laser speckle (**b**) in a typical animal can be seen over the right hemisphere 60 min after MCA occlusion. The distance between the LD probe and the chosen ROI (circle on the LSF images) is about 6 mm. The elapsed time between the flow spikes is about 100 sec, and the calculated velocity of PIFT is 3.6 mm/min. Relative timing of the color images (c–f) is indicated at upper left. [Color figure can be viewed in the online issue, which is available at www.interscience.wiley.com.]

Higher positive peaks were also characteristic for this area (Table II). The hyperemic flow changes represent 45.7% (181/396) of all events.

Types II, III: Biphasic Flow Transients

This pattern—transient decrease in perfusion followed by an increase (Fig. 5)—is characteristic for the first event (anoxic depolarization; 60%). During ischemia, this type appears evenly over the entire monitored cortex (Table III). We distinguished both hyperemia (II)- and hypoperfusion (III)-dominant forms based on whether the flow increase or the decrease contributed more than 50% to the amplitude. The first component of a biphasic transient was always hypoperfusion, followed by hyperemia. We did not find significant differences in the mean pretransient baseline flow between these two subgroups (43% ± 15% (II) vs. 41% ± 12%

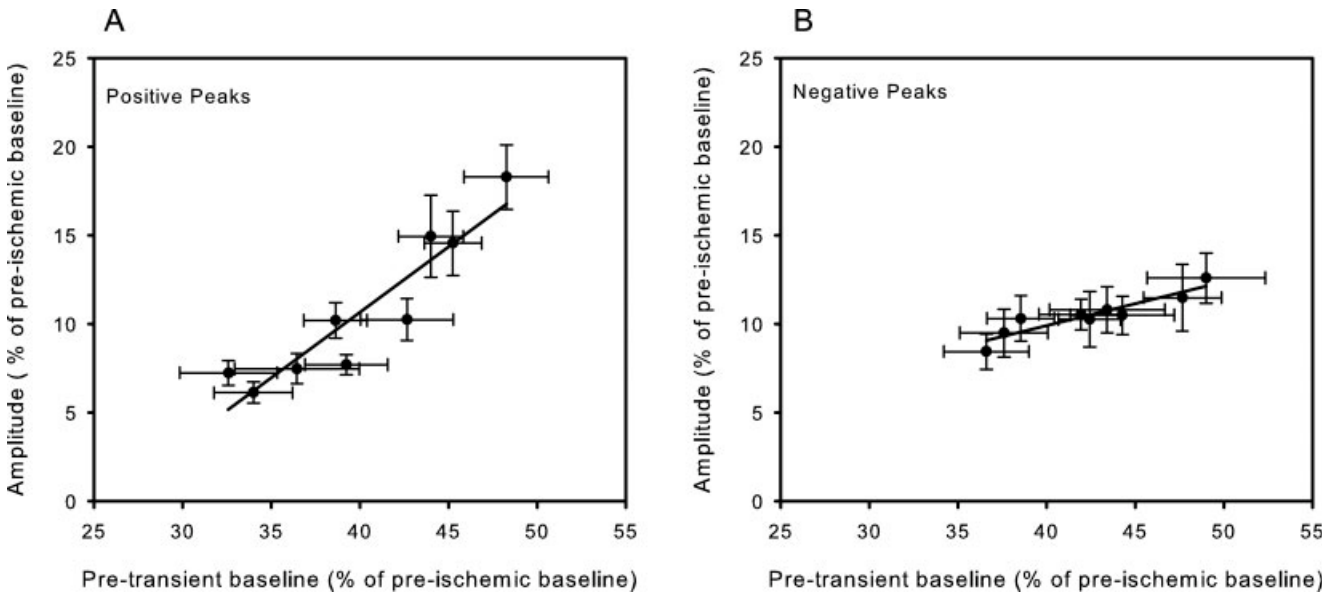

Fig. 4. Relationship between pretransient baseline and the positive (**A**) and negative (**B**) peak amplitudes. Data points are derived from the nine regions of interest shown in Figure 1. A: Linear regression analysis shows a positive correlation between the positive peaks and the pretransient baseline ($r^2 = 0.92$, $P < 0.001$). B: Line of regression was also obtained for negative peaks and pretransient baseline ($r^2 = 0.92$, $P < 0.001$). Error bars represent mean ± SEM of both the baseline and the amplitudes.

(III), *t*-test, $P = 0.37$). The biphasic patterns (II, III) represent 33.3% (132/396) of all events. Similarly, their occurrence over ROI 1–6 is 35.2% (93/264).

Types IV, V: Monophasic, Hypoperfusive Flow Transients

Falls in perfusion associated with a propagating event (Fig. 5) but not followed by relative hyperemia were most common (16–31%) on the anterolateral part of the MCA territory (ROI 1, 2, 4, 5; Table III). The occurrence of types IV and V was greater over the lateral row than over the most medial row (ROI 7–9; $P < 0.01$). This type was found in 9 of 10 animals, but in two of these animals the following flow transients were hyperemic over the same region of interest, so the appearance of the hypoperfusive response was ''reversible.'' In the transient type IV, the flow recovered within 2–3 min, whereas, in type V, there was no full flow recovery. The hypoperfusive flow changes (types IV and V) represent only 14.9% (59/396) of all events, although this figure is 18.6% (49/264) over ROI 1–6. Interestingly, this value is 31% over ROI 4 (the closest point to LD), much higher than that seen with LD (10.9%).

Propagation Pattern of PIFTs

The PIFTs propagated with a velocity of 3.1 ± 1.0 mm/min, usually in a rostral-caudal direction (except one event when the propagation was caudal-rostral). The types (I–V) of the flow changes showed great regional heterogeneity (Fig. 6) during the propagation of the PIFTs, but we were unable to group these types into well-defined propagation patterns.

LD Flowmetry

MCA occlusion resulted in an immediate reduction of CBF to 20% ± 6% of baseline in the territory supplied by the ipsilateral MCA. The blood flow remained relatively constant over the 90 min of occlusion (29% ± 9%), rising to 118% ± 46% in the reperfusion phase. PIFTs as detected by LD occurred in all the rats. The mean number of PIFTs was 4.6 ± 1.8, with a mean duration of 162 ± 34 sec (Table II). We excluded only one ''false'' (hyperemia-like) PIFT because of unstable blood pressure. (The flow change completely mirrored the sharp changes in blood pressure and did not show a propagating feature by LS.) The amplitudes of the positive and negative peaks were comparable with the results from LS (Table II). The first flow transients occured 227 ± 15 sec after MCA occlusion over the site of the LD and approximately one-half of the first flow transients (anoxic depolarization) were hyperemic and one-half were biphasic. The wave morphology of all PIFTs recorded by LD was prominently hyperemic (71.7%), with only 10.9% and 17.4% of the flow transients hypoperfusive or biphasic.

Neurological Score and Histology

The neurobehavioral score had a mean of 9.2 ± 1.0 at 72 hr. Temporary MCA occlusion produced his-

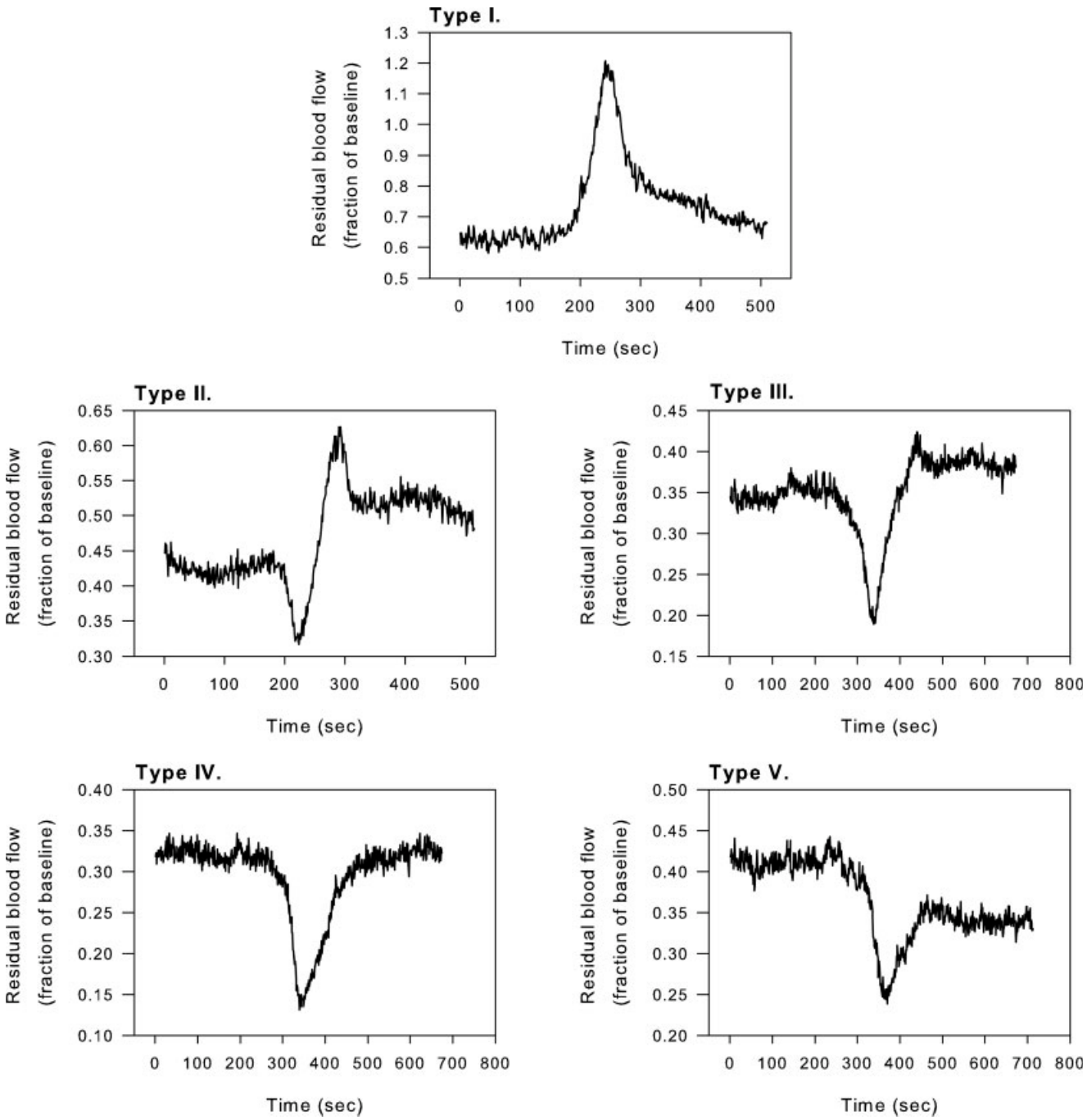

Fig. 5. Five different types of flow transients can be seen. The residual CBFs are shown at left and the elapsed time at bottom. Type I: a monophasic, hyperemic flow transient, typical of the periischemic area (ROI 7–9). Types II, III: biphasic flow transients characteristic of the first event (anoxic depolarization). Later, this type appears over the entire cortex. Types IV, V: monophasic, hypoperfusive flow transients, typical of the anterior part of the MCA territory (ROI 1, 2, 4, 5). Time scales are different in the different panels.

tological damage both in the cortex (infarct volume 124 ± 20 mm^3) and in the striatum (55 ± 10 mm^3). A positive correlation was found between the extent of the reactive hyperemia measured by LD during the early (1–15 min) reperfusion period and the cortical infarct size ($P = 0.035$), but the correlation between reperfusion as measured with LS and infarct size failed to achieve significance.

TABLE III. Number and Occurrence (percentage) of Different Types (I–V) of PIFTs Over Different ROIs*

ROI 4			ROI 5			ROI 6		
Type	Number	%	Type	Number	%	Type	Number	%
I	17	39	I	13	30	I	19	43
II	5	11	II	8	18	II	10	23
III	4	9	III	7	16	III	7	16
IV	5	11	IV	6	14	IV	2	5
V	9	20	V	6	14	V	3	7
N.I.	4	9	N.I.	4	9	N.I.	3	7
ROI 1			ROI 2			ROI 3		
Type	Number	%	Type	Number	%	Type	Number	%
I	13	30	I	17	39	I	22	50
II	10	23	II	7	16	II	9	20
III	9	20	III	9	20	III	8	18
IV	5	11	IV	3	7	IV	3	7
V	3	7	V	4	9	V	0	0
N.I.	4	9	N.I.	4	9	N.I.	2	5
ROI 7			ROI 8			ROI 9		
Type	Number	%	Type	Number	%	Type	Number	%
I	24	55	I	28	64	I	28	64
II	12	27	II	9	20	II	8	18
III	3	7	III	4	9	III	3	7
IV	4	9	IV	3	7	IV	3	7
V	0	0	V	0	0	V	0	0
N.I.	1	2	N.I.	0	0	N.I.	2	5

*The occurrence of type I (hyperemic) is remarkably higher over the periischemic area (ROI 7, 8, 9) than over the anterior part of the MCA territory (ROI 1, 2, 4, 5). The posterior region of the MCA (ROI 3, 6) has a slightly higher occurrence of type I than the anterior region, presumably because it is closer to the vertebrobasilar territory. The occurrence of the hypoperfusive flow transients (types IV, V) shows an inverse distribution compared with type I. The distribution of the biphasic PIFTs seems to be more random. The occurrence of nonidentifiable events (N.I.) over the periischemic area (ROI 7, 8, 9) is less frequent than over the ischemic cortex (ROI 1–6).

DISCUSSION

Our study provides combined LS and LD data on PIFTs in the rat in a closed-skull preparation. The LS data show that PIFTs can change their morphology over the ischemic and periischemic cortex (regional heterogeneity). We presume that the parameters (amplitude, morphology) of the flow transients may serve as a hemodynamic/functional biomarker of the underlying cortex, but this has to be tested in other ischemia models (permanent, distal MCA occlusion, thromboembolic, etc.) along with monitoring of metabolic changes.

Introduction of the LS method for imaging of cerebral cortical perfusion has provided a means of monitoring cortical perfusion with excellent temporal and spatial resolution (Dunn et al., 2001). We chose the filament occlusion model to keep the skull and the dura intact in order to minimize the chance of producing SDs during the surgical preparation, which can trigger stroke preconditioning (Kariko et al., 1998), can release vasoactive substances (Gold et al., 1998; Reuter et al., 1998), and can impair the vascular reactivity (Seitz et al., 2004; Scheckenbach et al., 2006).

Contrary to our original hypothesis, this study provides another example, this time in the rat, that PIFTs are highly polymorphic when monitored with LS. Similar to the results of Strong and colleagues (2007) in cats, five different patterns of flow transients were observed here. Shin and colleagues (2006) also reported a polymorphism of PIFTs in a distal MCA occlusion in mice. Insofar as the flow transients are solely hypoperfusive over the ischemic cortex in the mouse study, our findings are more comparable to the results obtained in cats (proximal MCAO), in which both biphasic and hyperemic events were seen over different parts of the penumbra. The differences could be attributed to the application of different ischemia models (distal MCA vs. proximal MCA occlusion) or species differences between rat and mouse. Although a species difference has been reported in the propagation of SD between mice and rats (Ayata et al., 2004), a similar comparison during ischemia has not been made. Because there are even substantial differences in ischemic lesion evolution between Sprague-Dawley and Wistar rats (Bardutzky et al., 2005), we presume that interstrain differences may exist in the propagation of flow transients.

The ischemia model used in different studies can also make a difference in the interpretation of the data. Distal occlusion of the MCA in mice produces an ischemic core in the cortex, which propagates to the penumbral area and causes a finely delineated gradient of residual CBF (Dunn et al., 2001). In rat distal MCA occlusion, a cyclic propagation of PIDs around the ischemic core has been reported (Graf et al., 2007). However, during filament occlusion (proximal) of the MCA in the rat, the striatum represents the ''ischemic core,'' with minimal postocclusion blood flow (Bardutzky et al., 2005), which later propagates to the cortex (Shen et al., 2005). In cat proximal MCA occlusion, a radial pattern of propagation (from core to periphery) has been observed during the early phase of ischemia, but later flow transients tangential to the core appear in clusters (Graf et al., 2007). Similarly, Hartings and colleagues (2003) report a rostral-caudal, caudal-rostral, and lateral-medial pattern of PID propagation in filament MCA occlusion model in the rat, in accordance with data from our laboratory for this model (unpublished data). The tangential, lateral-medial and caudal-rostral propagation of PIDs and flow transients suggests that these are also circulating (presumably after the core involves the cortex), but only a fraction of this cycle can be seen because of methodological limitations.

Studying periinfarct depolarizations or flow transients may give us a better understanding of stroke pathomechanism and evolution, but in addition the regional heterogeneity and polymorphism of the flow transients potentially could serve as hemodynamic/functional biomarkers of the underlying cortex. The higher residual blood flow and amplitude of flow transients along with the larger percentage of hyperemic (type I) flow transients in the medial ROIs indicates that this region repre-

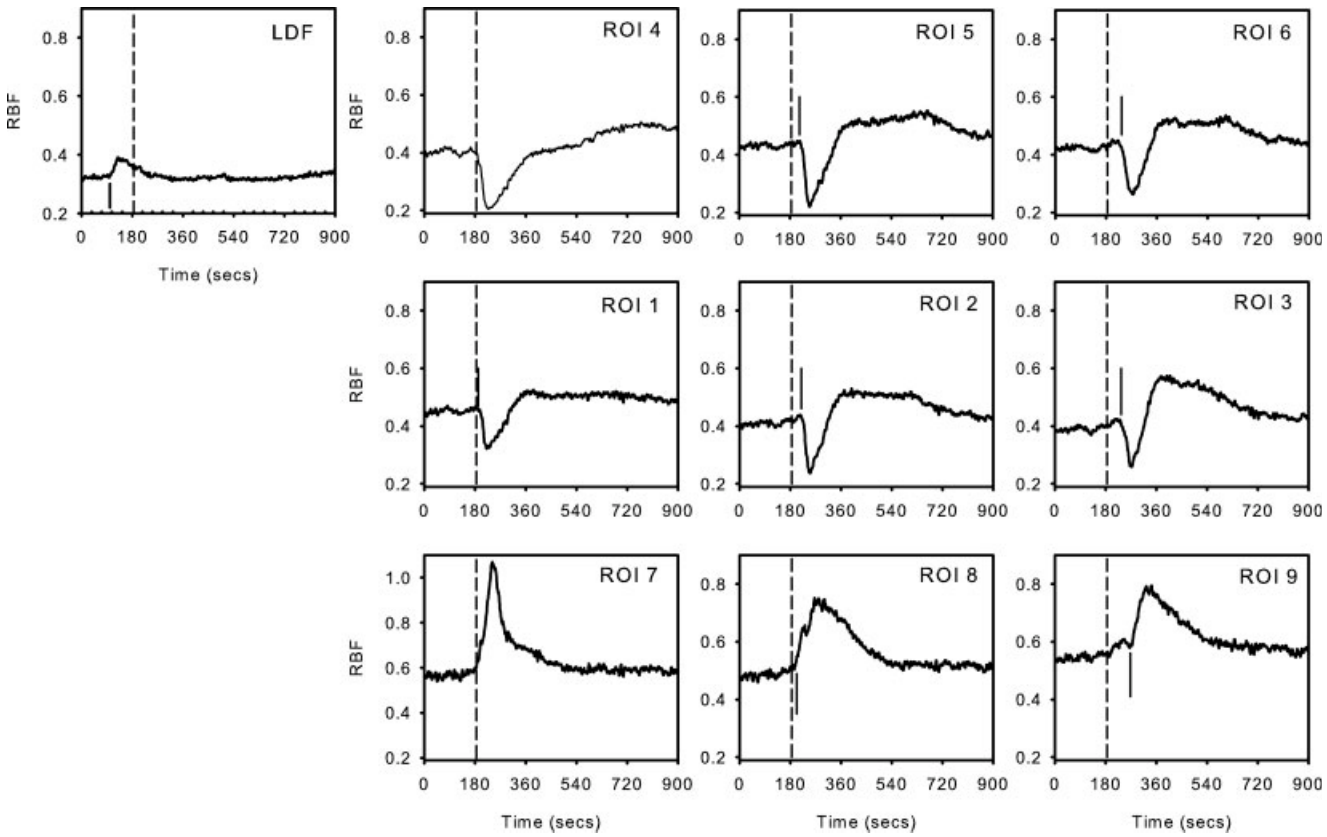

Fig. 6. Example of spatial heterogeneity of a propagating periinfarct flow transient (PIFT). Each panel shows the change in flow over the nine ROIs as well as from the laser Doppler site (see Fig. 1). Whereas the periischemic area is dominated by hyperemic flow changes (type I) with larger amplitude, the hypoperfusive (type IV) and hypoperfusion-dominant biphasic flow changes (type III) are characteristic of the lateral, anterolateral areas. This propagation pattern is representative of only 12 of 46 of the PIFTs. Note the rostral-caudal propagation of the PIFT. The dotted line marks the beginning of the PIFT in ROI 4 and is reproduced in all panels to show the propagation. The short solid lines indicates the actual time of deflection in each ROI. Note that the deflection at the LDF site precedes that in the laser speckle ROIs.

sents the watershed zone between the MCA and the ACA territories (stealing through collaterals). The frequent reversals of blood flow in arterioles at the periphery of the MCA territory in the same ischemia model demonstrate that arteriolar anastomoses are functional (Pinard et al., 2002). In contrast, lower residual flow and smaller amplitudes with higher percentage of hypoperfusive flow transients (types IV, V) are characteristic for the ''pure'' MCA territory (ROI 1–6). In addition, a positive correlation was found between amplitude and pretransient baseline over each ROI. We conclude that the parameters, especially the amplitudes of the PIFTs and partially the morphology, are good indicators of the hemodynamic reserve (residual blood flow, collateral supply via the anastomotic network) of the underlying cortex. Although we did not perform metabolic measurements and induced only 90 min of ischemia, we speculate that hypoperfusive flow transients (types IV, V) may indirectly indicate the propagation of the core, because they first appear over the cortex only 36 ± 16 min after the occlusion, occur with higher frequency over the anterolateral areas of the MCA, and seemed to be reversible (later followed by a biphasic or hyperemic events) only in two animals.

There are suggestions in the literature that the flow morphology related to depolarizations is also determined by active vasoconstrictor mechanisms. Our observation that hypoperfusion always precedes hyperemia is supported by these data and is in agreement with the results of Strong and colleagues (2007). Thus it is likely that the different flow morphologies reflect changes in regulation of the neurovascular unit during ischemia. Endothelin-1, a powerful cerebral vasoconstrictor, elicits SD when applied locally (Dreier et al., 2002). Several papers report increased hypoperfusion in response to elevated potassium or SD in the presence of nitric oxide (NO) synthase inhibition (Dreier et al., 1995; Fabricius et al., 1995; Ayata et al., 2004), which is consistent with the hypothesis that NO levels might determine the response to depolarization (Metea and Newman, 2006).

Although the LD and LS measurements were made over different parts of the MCA territory (the closest

points were 3–4 mm apart), the mean duration and number of PIFTs were the same, with 95.6% of them time correlated. The positive and negative PIFT peaks measured with LD were very similar to the values over the lateral and middle rows of ROIs (ROI 1–6) as monitored with LS. Because the flow transients were well ''coupled'' and their parameters (duration, amplitudes) were almost identical with these two methods, both LS with its excellent spatial-temporal resolution and LD are suitable tools for monitoring and assessing PIFTs.

Differences in residual blood flow and the occurrence of different PIFT morphologies were also observed with these two methods. The mean flow during 90 min of ischemia in our series was 29% ± 9% by LD compared with 36% ± 10% to 42% ± 10% (depending on the ROI) by LS over the anterolateral area, which is the closest territory to the LD recording site. Surprisingly, the flow transients as measured by LD are more hyperemic than those measured by LS, with 71.7% of the flow transients characterized by a monophasic increase of flow, 17.4% being biphasic, and only 10.9% being hypoperfusive. This is consistent with previous studies in our laboratory in rats subject to filament occlusion anesthetized with halothane, isoflurane, or α-chloralose (unpublished data). Regional (tangential) heterogeneity in residual CBF and morphology might account for these differences, insofar as a similar phenomenon has been observed during mild hypotension (Kharlamov et al., 2004) and the application of endothelin-1 (Dreier et al., 2007). Although our LS data support the existence of regional (tangential) heterogeneity in the morphology of the propagating flow transients, our LD data look different. In a previous study in which two LD probes were placed over the rostral and caudal part of the MCA territory, the proportions of flow morphologies were identical over the two probes (unpublished observations) and comparable to the morphology seen in the present study. It is also unlikely that the difference in the ischemic flow (LD = 29%, LS = 36–42%) can be explained by the ROIs of the LS being closer to the posterior circulation thanb those of the LD, since there was no increasing rostral-caudal flow gradient seen with LS. However, it is possible that these differences are due to potential differences in depth sensitivity of these two methods, and a laminar (vertical) heterogeneity may exist in the propagation of the flow transients. Dunn and colleagues (2001) found a high correlation between LD and LS under conditions of SD and ischemia in rats, whereas other studies have shown some discrepancies (Durduran et al., 2004; Kharlamov et al., 2004; Royl et al., 2006). Laminar specificity during somatosensory stimulation imaged by fMRI (Silva and Koretsky, 2002) or autoradiography (Gerrits et al., 2000) or during SD by LD flowmetry (Fabricius et al., 1997) has been observed in rat. Using a laser with wavelength 780 nm and a 250 μm fiber separation Fabricius et al. (1997) found that 47% of the signal comes from the most superficial 0.25 mm, with 22% coming for the next 0.25 mm and 31% from tissue between 0.5 mm and 1.0 mm (containing layer IV), consistent with Monte-Carlo simulations of LD flowmetry, which indicate that the median sampling depth is approximately 550 μm (Jakobsson and Nilsson, 1993). We speculate that LS scans the shallower cortical layers (<500 μm), but, unfortunately, no one has ever made a quantitative depth sensitivity analysis for LS.

In conclusion, this study shows that there is significant regional heterogeneity in PIFTs in the ischemic and periischemic cortex of the rat during filament occlusion of the MCA. The polymorphism of the PIFTs may serve as a biomarker of the underlying cortex.

REFERENCES

Ayata C, Shin HK, Salomone S, Ozdemir-Gursoy Y, Boas DA, Dunn AK, Moskowitz MA. 2004. Pronounced hypoperfusion during spreading depression in mouse cortex. J Cereb Blood Flow Metab 24:1172–1182.

Bandyopadhyay R, Gittings AS, Suh SS, Dixon PK, Durian DJ. 2005. Speckle-visibility spectroscopy: tool to study time-varying dynamics. Rev Sci Instrument 76:093110.

Bardutzky J, Shen Q, Henninger N, Bouley J, Duong TQ, Fisher M. 2005. Differences in ischemic lesion evolution in different rat strains using diffusion and perfusion imaging. Stroke 36:2000–2005.

Belayev L, Alonso OF, Busto R, Zhao W, Ginsberg MD. 1996. Middle cerebral artery occlusion in the rat by intraluminal suture. Neurological and pathological evaluation of an improved model. Stroke 27:1616–1622.

Branston NM, Strong AJ, Symon L. 1977. Extracellular potassium activity, evoked potential and tissue blood flow. Relationships during progressive ischaemia in baboon cerebral cortex. J Neurol Sci 32:305–321.

Briers JD. 2001. Laser Doppler, speckle and related techniques for blood perfusion mapping and imaging. Physiol Meas 22:R35–R66.

Burnett MG, Shimazu T, Szabados T, Muramatsu H, Detre JA, Greenberg JH. 2006. Electrical forepaw stimulation during reversible forebrain ischemia decreases infarct volume. Stroke 37:1327–1331.

Dreier JP, Korner K, Gorner A, Lindauer U, Weih M, Villringer A, Dirnagl U. 1995. Nitric oxide modulates the CBF response to increased extracellular potassium. J Cereb Blood Flow Metab 15:914–919.

Dreier JP, Petzold G, Tille K, Lindauer U, Arnold G, Heinemann U, Einhaupl KM, Dirnagl U. 2001. Ischaemia triggered by spreading neuronal activation is inhibited by vasodilators in rats. J Physiol 531:515–526.

Dreier JP, Kleeberg J, Petzold G, Priller J, Windmuller O, Orzechowski HD, Lindauer U, Heinemann U, Einhaupl KM, Dirnagl U. 2002. Endothelin-1 potently induces Leao's cortical spreading depression in vivo in the rat: a model for an endothelial trigger of migrainous aura? Brain 125:102–112.

Dreier JP, Kleeberg J, Alam M, Major S, Kohl-Bareis M, Petzold GC, Victorov I, Dirnagl U, Obrenovitch TP, Priller J. 2007. Endothelin-1-induced spreading depression in rats is associated with a microarea of selective neuronal necrosis. Exp Biol Med 232:204–213.

Dunn AK, Bolay H, Moskowitz MA, Boas DA. 2001. Dynamic imaging of cerebral blood flow using laser speckle. J Cereb Blood Flow Metab 21:195–201.

Durduran T, Burnett MG, Yu G, Zhou C, Furuya D, Yodh AG, Detre JA, Greenberg JH. 2004. Spatiotemporal quantification of cerebral blood flow during functional activation in rat somatosensory cortex using laser-speckle flowmetry. J Cereb Blood Flow Metab 24:518–525.

Fabricius M, Akgoren N, Lauritzen M. 1995. Arginine-nitric oxide pathway and cerebrovascular regulation in cortical spreading depression. Am J Physiol 269:H23–H29.

Fabricius M, Akgoren N, Dirnagl U, Lauritzen M. 1997. Laminar analysis of cerebral blood flow in cortex of rats by laser-Doppler flowmetry: a pilot study. J Cereb Blood Flow Metab 17:1326–1336.

Gerrits RJ, Raczynski C, Greene AS, Stein EA. 2000. Regional cerebral blood flow responses to variable frequency whisker stimulation: an autoradiographic analysis. Brain Res 864:205–212.

Goadsby PJ, Kaube H, Hoskin KL. 1992. Nitric oxide synthesis couples cerebral blood flow and metabolism. Brain Res 595:167–170.

Gold L, Back T, Arnold G, Dreier J, Einhaupl KM, Reuter U, Dirnagl U. 1998. Cortical spreading depression-associated hyperemia in rats: involvement of serotonin. Brain Res 783:188–193.

Goodman J. 1985. Statistical optics. Hoboken, NJ: John Wiley & Sons.

Graf R, Nakamura H, Vollmar S, Dohmen C, Sakowitz B, Bosche B, Dunn AK, Strong AJ. 2007. Cycling propagation of spontaneous spreading depolarizations around ischemic foci: evidence from experimental and clinical assessments. Society of Neuroscience, San Diego, CA Program No. 7659.

Hartings JA, Rolli ML, Lu XC, Tortella FC. 2003. Delayed secondary phase of peri-infarct depolarizations after focal cerebral ischemia: relation to infarct growth and neuroprotection. J Neurosci 23:11602–11610.

Hossmann KA. 1996. Periinfarct depolarizations. Cerebrovasc Brain Metab Rev 8:195–208.

Iijima T, Mies G, Hossmann KA. 1992. Repeated negative DC deflections in rat cortex following middle cerebral artery occlusion are abolished by MK-801: effect on volume of ischemic injury. J Cereb Blood Flow Metab 12:727–733.

Jakobsson A, Nilsson GE. 1993. Prediction of sampling depth and photon pathlength in laser Doppler flowmetry. Med Biol Eng Comput 31:301–307.

Kariko K, Harris VA, Rangel Y, Duvall ME, Welsh FA. 1998. Effect of cortical spreading depression on the levels of mRNA coding for putative neuroprotective proteins in rat brain. J Cereb Blood Flow Metab 18:1308–1315.

Kharlamov A, Brown BR, Easley KA, Jones SC. 2004. Heterogeneous response of cerebral blood flow to hypotension demonstrated by laser speckle imaging flowmetry in rats. Neurosci Lett 368:151–156.

Leao AAP, Dusser de Barenne JG, Fulton JF, Gerard RW. 1944. Pial circulation and spreading depression of activity in the cerebral cortex. J Neurophysiol 7:391–396.

Luckl J, Keating J, Greenberg JH. 2008. Alpha-chloralose is a suitable anesthetic for chronic focal cerebral ischemia studies in the rat: a comparative study. Brain Res 1191:157–167.

Metea MR, Newman EA. 2006. Glial cells dilate and constrict blood vessels: a mechanism of neurovascular coupling. J Neurosci 26:2862–2870.

Nallet H, MacKenzie ET, Roussel S. 2000. Haemodynamic correlates of penumbral depolarization following focal cerebral ischaemia. Brain Res 879:122–129.

Parthasarathy AB, Tom WJ, Gopal A, Zhang X, Dunn AK. 2008. Robust flow measurements with multi-exposure speckle imaging. Optics Express 16.

Paxinos G, Watson C. 1982. The rat brain in stereotaxic coordinates. San Diego: Academic Press.

Pinard E, Nallet H, MacKenzie ET, Seylaz J, Roussel S. 2002. Penumbral microcirculatory changes associated with peri-infarct depolarizations in the rat. Stroke 33:606–612.

Reuter U, Weber JR, Gold L, Arnold G, Wolf T, Dreier J, Lindauer U, Dirnagl U. 1998. Perivascular nerves contribute to cortical spreading depression-associated hyperemia in rats. Am J Physiol 274:H1979–H1987.

Royl G, Leithner C, Sellien H, Muller JP, Megow D, Offenhauser N, Steinbrink J, Kohl-Bareis M, Dirnagl U, Lindauer U. 2006. Functional imaging with laser speckle contrast analysis: vascular compartment analysis and correlation with laser Doppler flowmetry and somatosensory evoked potentials. Brain Res 1121:95–103.

Scheckenbach KE, Dreier JP, Dirnagl U, Lindauer U. 2006. Impaired cerebrovascular reactivity after cortical spreading depression in rats: Restoration by nitric oxide or cGMP. Exp Neurol 202:449–455.

Seitz I, Dirnagl U, Lindauer U. 2004. Impaired vascular reactivity of isolated rat middle cerebral artery after cortical spreading depression in vivo. J Cereb Blood Flow Metab 24:526–530.

Shen Q, Ren H, Cheng H, Fisher M, Duong TQ. 2005. Functional, perfusion and diffusion MRI of acute focal ischemic brain injury. J Cereb Blood Flow Metab 25:1265–1279.

Shimazu T, Inoue I, Araki N, Asano Y, Sawada M, Furuya D, Nagoya H, Greenberg JH. 2005. A peroxisome proliferator-activated receptor-gamma agonist reduces infarct size in transient but not in permanent ischemia. Stroke 36:353–359.

Shin HK, Dunn AK, Jones PB, Boas DA, Moskowitz MA, Ayata C. 2006. Vasoconstrictive neurovascular coupling during focal ischemic depolarizations. J Cereb Blood Flow Metab 26:1018–1030.

Silva AC, Koretsky AP. 2002. Laminar specificity of functional MRI onset times during somatosensory stimulation in rat. Proc Natl Acad Sci U S A 99:15182–15187.

Strong AJ, Venables GS, Gibson G. 1983. The cortical ischaemic penumbra associated with occlusion of the middle cerebral artery in the cat: 1. Topography of changes in blood flow, potassium ion activity, and EEG. J Cereb Blood Flow Metab 3:86–96.

Strong AJ, Bezzina EL, Anderson PJ, Boutelle MG, Hopwood SE, Dunn AK. 2006. Evaluation of laser speckle flowmetry for imaging cortical perfusion in experimental stroke studies: quantitation of perfusion and detection of peri-infarct depolarisations. J Cereb Blood Flow Metab 26:645–653.

Strong AJ, Anderson PJ, Watts HR, Virley DJ, Lloyd A, Irving EA, Nagafuji T, Ninomiya M, Nakamura H, Dunn AK, Graf R. 2007. Peri-infarct depolarizations lead to loss of perfusion in ischaemic gyrencephalic cerebral cortex. Brain 130:995–1008.

Sukhotinsky I, Dilekoz E, Moskowitz MA, Ayata C. 2008. Hypoxia and hypotension transform the blood flow response to cortical spreading depression from hyperemia into hypoperfusion in the rat. J Cereb Blood Flow Metab 28:1369–1376.

Wang Z, Hughes S, Dayasundara S, Menon RS. 2007. Theoretical and experimental optimization of laser speckle contrast imaging for high specificity to brain microcirculation. J Cereb Blood Flow Metab 27: 258–269.

Zhou C, Shimazu T, Durduran T, Luckl J, Kimberg DY, Yu G, Chen XH, Detre JA, Yodh AG, Greenberg JH. 2008. Acute functional recovery of cerebral blood flow after forebrain ischemia in rat. J Cereb Blood Flow Metab 28:1275–1284.